



Parametric analysis of a zero-energy building aiming for a reduction of CO₂ emissions for warm climate

Mohsen Mahdavi Adeli¹ · Said Farahat¹ · Faramarz Sarhaddi¹

Received: 6 September 2019 / Accepted: 26 May 2020 / Published online: 16 June 2020
© Springer-Verlag GmbH Germany, part of Springer Nature 2020

Abstract

Considering the reduction of fossil fuel resources and the increase of environmental pollutions, everyone is aware of the importance of saving on consumption of energies generated from fossil fuels. Global statistics demonstrates that 30–40% of the energy across different countries worldwide is used in residential buildings. Therefore, one way of efficiency and optimization of energy consumption is to construct buildings that consume the least energy for heating and cooling. Aiming for the analysis of the total amount of annual energy required for heating and cooling, this research was conducted in a combined novel method (simulation and descriptive-analytic) on four samples of a two-story building, simulated in Design Builder Software in the four main directions of north, east, south, and west by using the weather data of warm climate, seeking the optimum orientation and ranking of the said buildings based on CO₂ emissions. The research results show that among the four sample buildings, the east-facing building ranked first with the minimum CO₂ emissions and the west-facing building won second place in the window to wall ratio (WWR) of 40%. Also, the building in a hot climate was considered, since it produced CO₂ annually 12,633 kg. No significant change is observed in the amount of CO₂ emissions in southeast, south, and southwest orientations, although smaller WWR (30% and 20%) is recommended for these three orientations.

Keywords Window to wall ratio (WWR) · Environmental emission · Energy consumption · Parametric design · Net-zero-energy building

Introduction

Many studies have been continuously conducted with the focus on energy-saving on buildings, and more research is needed for using renewable energies instead of using fossil fuels. Specifically, the infinite solar energy, among other green energies without territorial restrictions (unlike fossil energies), forms a focal point and research on its use in construction is continuously underway.

Cellat et al. conducted comprehensive, experimental, and numerical studies on the use of phase change materials (PCM) to improve and reduce energy consumption in sustainable buildings. They have studied PCMs in various forms (using

bio-based fatty acids such as PCM, microencapsulated PCM in concrete and butyl stearate) under different conditions and, in all cases have concluded that the use of PCM in buildings causes increased human thermal comfort and increased energy saving (Cellat et al. 2015, 2019; Beyhan et al. 2017). Mahdavi Adeli et al. after in-depth studies on optimizing energy consumption in the zero-energy buildings put forward various scenarios for using a zero-energy building for renewable energy and concluded that in hot climates, using a solar panel alone to achieve a zero-energy building is not enough, and wind turbines or other renewable energies should also be used (Mahdavi Adeli et al. 2017, 2019, 2020). They also conducted other extensive theoretical and experimental studies on the application of solar renewable energy in buildings (Sarhaddi et al. 2010; Mahdavi Adeli et al. 2011, 2012; Namjoo et al. 2011; Yazdanpanahi et al. 2015; Valizadeh et al. 2019).

For the effective use of this solar energy, the input radiation of buildings must be correctly controlled. As windows are the main outlet of a building for the entrance of solar radiations, they must be controlled for the increase of lighting, cooling, and heating energies while thermal comfort of occupants

Responsible editor: Philippe Garrigues

✉ Said Farahat
said.farahat.usb@gmail.com

¹ Department of Mechanical Engineering, University of Sistan and Baluchestan, Zahedan, Iran

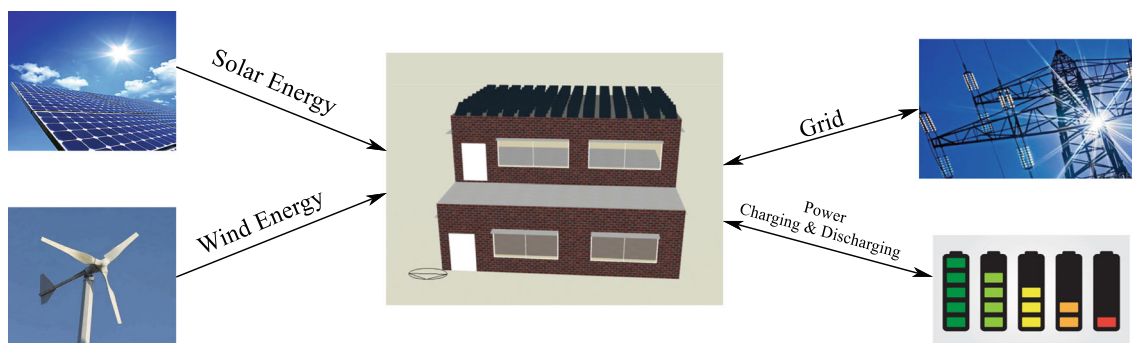


Fig. 1 Energy exchange of the modeled building with renewable resources and grid

should also be provided (Feng et al. 2017; Syngros et al. 2017; Kwon et al. 2018; Petrichenko et al. 2019). Su et al. studied the proper WWR range for different building orientations and the material of windows in an office building in Shanghai, China. While studying the effects of building appearance, they reached the conclusion that by increasing the WWR, a small but significant (around 5–9%) decrease occurs in adverse environmental impacts (Su and Zhang 2010). Stavrakakis et al. studied a natural cross-ventilated building in hot climate experimentally and numerically. The computational fluid dynamics (CFD) model of their building was developed and then they conducted studies with two various thermal comfort models at high-temperature experimental conditions. They concluded that all the turbulence simulation models were used in good agreement with their experimental results (Stavrakakis et al. 2008). Azari et al. addressed the impacts of window type, window frame materials, thermal resistance of walls, ratio of windows to south-facing and north-facing walls, and insulation materials in an office building, reaching the conclusion that the most optimum case for reduction of energy consumption and environmental emissions is a south WWR 60% and a north WWR 10% (Azari et al. 2016). Lobaccaro et al. used the parametric analysis aiming for the minimization of greenhouse gas emissions as well as the energy consumption in a zero-emission building, and using form optimization, they selected ten forms to utilize the potentials of solar energy (Lobaccaro et al. 2018). Charles et al. adopted

a parametric study to investigate the impact of wall and ceiling insulation, airtightness, and window replacement on an old office building in Vancouver, Canada, reaching the result that correcting them can reduce 45% of the total energy consumption and that reducing the use of natural gas helps save 70 tons of CO₂ emissions (Charles et al. 2018). Moschetti et al. addressed the most influential factors of environmental and economic problems in zero-energy and zero-emission buildings, proposing a way to solving these problems in buildings. One of their suggestions was widespread use of wood in constructions which would lead to about 30% reduction in global warming potential (GWP) (Moschetti et al. 2019). Pathirana et al. examined the impact of form, orientation, window to wall ratio, and zones on the consumption of lighting energy in about 300 different two-story buildings, with 24 orientations in warm climates with natural ventilation. They concluded that WWR changes had the largest effect on the thermal comfort of occupants (20–55%) compared with the electrical energy for lighting (1.5–9.5%) (Pathirana et al. 2019). Harmati et al. performed a detailed analysis on the optimization of the operation of energy consumption in existing office buildings by determination of window to wall ratio and geometry. The result of their study was indicative of the impact of glass parameters on the annual energy demand of the building (Harmati and Magyar 2015). Alwetaishi focused on exploring the window to wall ratios of 5%, 10%, 20%, 30%, and 40% in a building. Having obtained that south and east are the worst

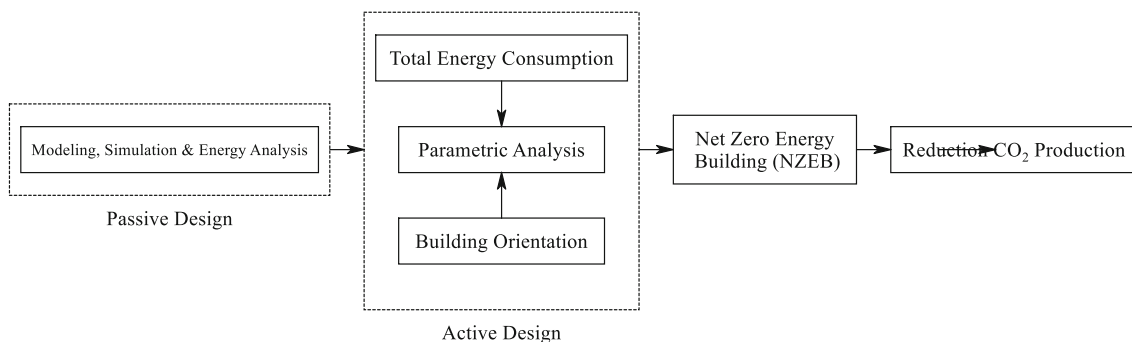


Fig. 2 The methodology and problem-solving strategy

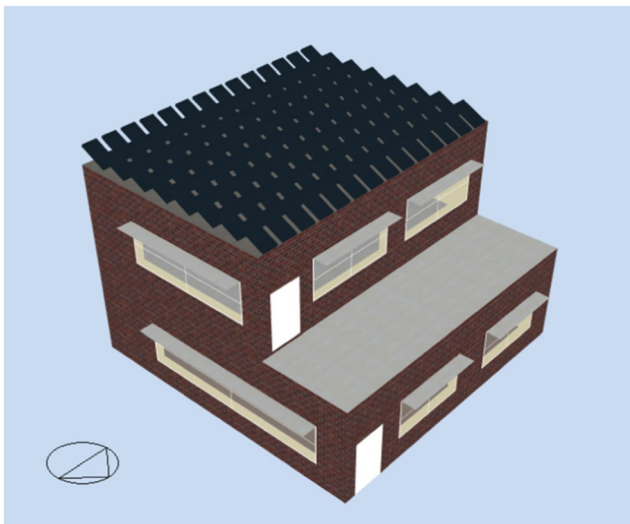


Fig. 3 The modeled building for analysis

orientations for heat collection, he proposed the WWR 10% for (both wet and dry) warm climate (Alwetaishi and Taki 2019). Zomorodian et al. studied a double skin façade (DSF) office building in which the maximum hours of thermal comfort and the minimum energy consumption for a warm and dry

Table 2 Building’s construction material

Layer no.	Material	Thickness (m)
1 (outer layer)	Brickwork outer	0.1
2 (middle layer)	Extruded polystyrene	0.0795
3 (middle layer)	Concrete block (medium)	0.1
4 (inner layer)	Gypsum plastering	0.0130

environment were observed, and they reached the result that energy consumption was reduced by 14.8%, and the operational carbon emission decreased up to 17%, while embodied carbon increased up to 47% (Zomorodian and Tahsildoost 2018).

Based on what has been said so far, although numerous studies have been carried out on the impact of different building orientations on the amount of energy consumption, but no comprehensive research has been conducted comparing the concurrent impacts of these parameters on the reduction of CO₂ emissions and embodied CO₂ in a warm and dry climate. It is mentionable that proper parameters for the said variables in envelopes should largely depend on the climate of the zone.

Table 1 Modeled building’s specification and site location

Parameters	Values/types
Program version	EnergyPlus, Version 8.6.0.001-c87e61b44b
Hours simulated (h)	8760
Weather file	Zahedan Airport - IRN ITMY WMO# = 408,210
Latitude (°)	29.48
Longitude (°)	60.91
Elevation about sea level (m)	1378
Site orientation (°)	0
HVAC	Ground source heat pump (GSHP) water to water heat pump, heated floor, chilled beams, nat vent
External walls U-value (W/m ² K)	0.350
Gross wall area (m ²)	259
Internal partitions U-value (W/m ² K)	1.639
Flat roof U-value (W/m ² K)	0.250
Internal floor U-value (W/m ² K)	2.929
Gross window to wall ratio (%)	19.55
Window opening area (m ²)	50.63
Glazing type	2 layers/air gap/13 mm
Windows shading	0.5 m/overhang
Lighting	Compact fluorescent (CFL)
Occupancy density (people/m ²)	0.111
Operating hours (h)	10 (8:00–18:00)
Activity of occupants	Light office work/standing/walking
Electricity density of office equipment (W/m ²)	11.77
Consumption rate of domestic hot water (DHW) (L/m ² day)	0.2

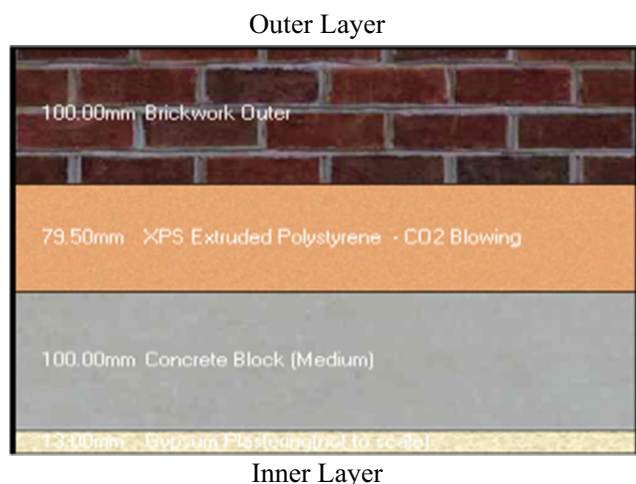


Fig. 4 The building wall cross-section

In other words, if a parameter leads to a decrease or increase in solar thermal collection, it will naturally result in a decrease or increase of the summer and winter load. Therefore, it is only possible to comment on the properness of the orientation and WWR of a building when the annual load for a certain climate is figured out. Unlike previous researches, in the present study, different techniques of reducing CO₂ emissions of a zero-energy building with the objective of reaching greater sustainability are investigated.

Methodology

Figure 1 demonstrates the use of renewable energies in the modeled building of the present study as well as how electrical energy is exchanged with the grid and the electricity storage device (battery). As can be seen in Fig. 1, the solar energy and wind energy are the constant generators of electrical current for the building. It should be noted that unlike the thermal energy, electrical energy cannot be easily stored after it is generated. For this problem, a battery is used after electricity is generated and converted into a storable form. In this study, the energy generation devices are connected to a battery,

Table 3 Photovoltaic panel specifications

Parameters	Values/types
Total area (m ²)	54
Fraction of surface with active PV	0.9
Efficiency (%)	15
Material	Bitumen felt
Heat transfer integration	Decoupled
Inverter efficiency (%)	90
Availability schedule	On 24/7

storing the electricity generated by them (after the electrical energy of the building is supplied), and if the battery becomes full, the surplus electricity is transferred to the overall electrical grid. Moreover, when the energy load of the building is large, the electrical energy stored in the battery is used first, and after the battery is fully discharged, electricity is received from the overall grid.

As shown in Fig. 2, all processes begin with building modeling and performing energy analysis and then optimization analysis to design a high-performance building. In the next step, solar and wind energy are added to the existing energy resources of the building and the results of their impact on the building are examined. It is important to note that in order to solve the current problem, the building must first be minimized in terms of internal energy consumption with proper building orientation, WWR, insulation, choice of building materials, etc. (passive design) and then increased energy production by renewable energy resources (active design). Using active design alone is not a suitable solution for zero-energy building design, meaning that increasing electricity generation by renewable energy sources to high-energy buildings is not a good strategy for achieving a zero-energy building. Finally, the parameters of net-zero-energy building are obtained by reducing the production of CO₂ emission.

Building model

A two-story building with office use in Zahedan City, Iran, with a total infrastructure of 149 m² and an occupied volume of 513 m³ was selected for this study. The 3D design of this building is illustrated in Fig. 3. Moreover, the design details of the modeled building are shown in Table 1.

In Table 2, the material used in the wall construction is considered. Since the aim is the lowest energy loss in the zero-energy building, the walls must be made of suitable insulation. As can be seen, the outer wall is made of brick with a thickness of 10 cm, and the inner layer is made of gypsum polyester. A schematic diagram of the section cut of this wall can be seen in Fig. 4.

As explained in the previous section, energy should be generated to supply part or all of energy consumption in a net-zero-emissions building. This generated energy consists of two general types of electrical and thermal energies. However, previous studies have shown that these energies can be converted to one another by some coefficients for the purpose of energy analysis in a mechanical system (Mahdavi Adeli et al. 2011; Mahdavi Adeli et al. 2019). As seen in Fig. 1, two types of photovoltaic solar and wind energies are used in this study to suit the climate potentials of Zahedan City. The specifications of the photovoltaic panel and the wind turbine used in the present study are stated in Tables 3 and 4, respectively.

Table 4 Wind turbine specifications

Parameters	Values/types
Rotor type	Horizontal axis wind turbine
Power control	Variable speed fixed pitch
Overall height (m)	11
Number of blades	3
Overall wind turbine system efficiency (%)	83.5
Availability schedule	On 24/7

Analysis of the total energy consumption

The most significant loads in a residential building are the cooling and heating loads. The total heat loss and heat gain in a building should be equal, as stated in Eq. 1 (EnergyPlus 2016):

$$\begin{aligned}
 -Q_{HVAC} &= Q_{\text{Total Site Energy Consumption}} \\
 &= \sum_{i=1}^{N_{sj}} \dot{Q}_i + \sum_{i=1}^{N_{\text{surface}}} h_i \cdot A_i \cdot (T_{si} - T_z) \\
 &\quad + \sum_{i=1}^{N_{\text{zones}}} m_i \cdot c_p \cdot (T_{zi} - T_z) + m_{\text{inf}} \cdot c_p \cdot (T_{\text{ext}} - T_z) \quad (1)
 \end{aligned}$$

In the above equation, $\sum_{i=1}^{N_{sj}} \dot{Q}_i$ is the total load resulted from the internal convective heat transfer, $\sum_{i=1}^{N_{\text{surface}}} h_i \cdot A_i \cdot (T_{si} - T_z)$ represents the convective heat exchange from surfaces of different zones, $\sum_{i=1}^{N_{\text{zones}}} m_i \cdot c_p \cdot (T_{zi} - T_z)$ is the heat transfer caused

by air combination in different zones, and $m_{\text{inf}} \cdot c_p \cdot (T_{\text{ext}} - T_z)$ is caused by heat transfer due to infiltration.

Heat transfer caused by the building components will impact the temperature of internal surfaces (T_{si}), and hence, Eq. 2 demonstrates the convective heat transfer between building surfaces and the internal air:

$$-q''_{\text{conv}} = q''_{LWX} + q''_{SW} + q''_{LWS} + q''_{\text{sol}} + q''_{ki} \quad (2)$$

where q''_{LWX} represents the flux of radiative heat transfer between surfaces with long wavelengths, q''_{SW} shows the flux of radiative heat transfer between lights and surfaces, and q''_{LWS} is the flux of radiative heat transfer between surfaces and radiants. Moreover, q''_{sol} and q''_{ki} represent the solar radiative flux and conductive heat transfer from the building surroundings, respectively. q''_{ki} can be figured out using Eq. 3:

$$\begin{aligned}
 q''_{ki}(t) &= -Z_o T_{i,t} - \sum_{j=1}^{nz} Z_j T_{i,t-j\delta} + Y_o T_{o,t} + \sum_{j=1}^{nz} Y_j T_{o,t-j\delta} \\
 &\quad + \sum_{j=1}^{nq} \psi_j q''_{ki,t-j\delta} \quad (3)
 \end{aligned}$$

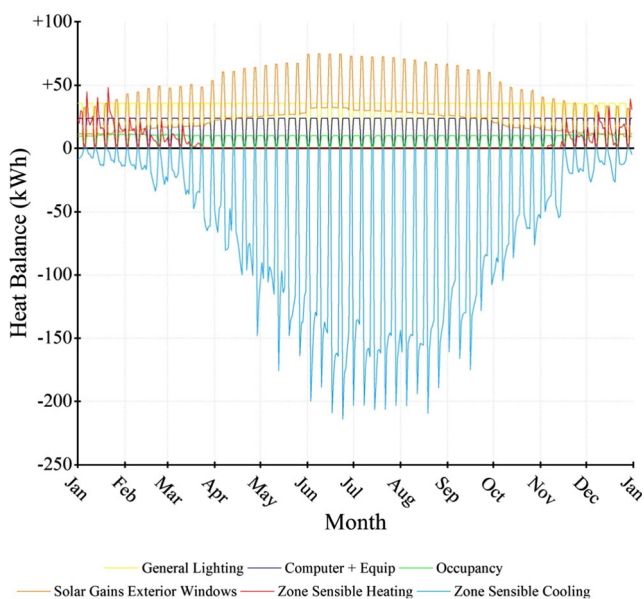


Fig. 5 Daily consumed energy of the building within a year

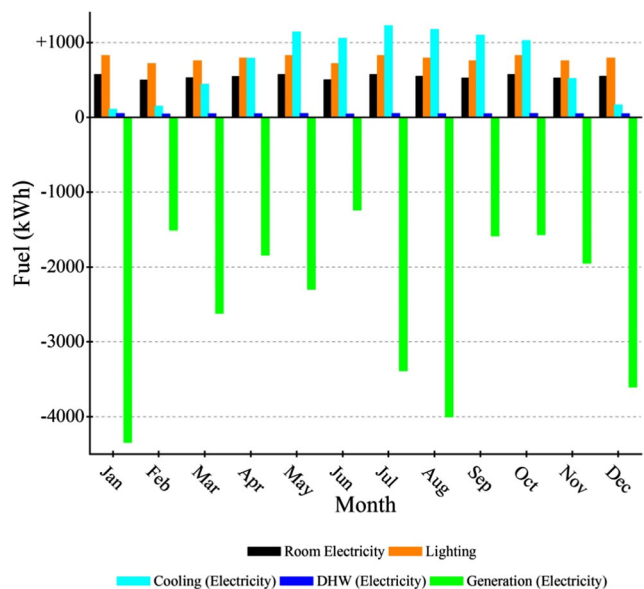


Fig. 6 Monthly energy generation and energy consumption using renewable energies in the zero-energy building

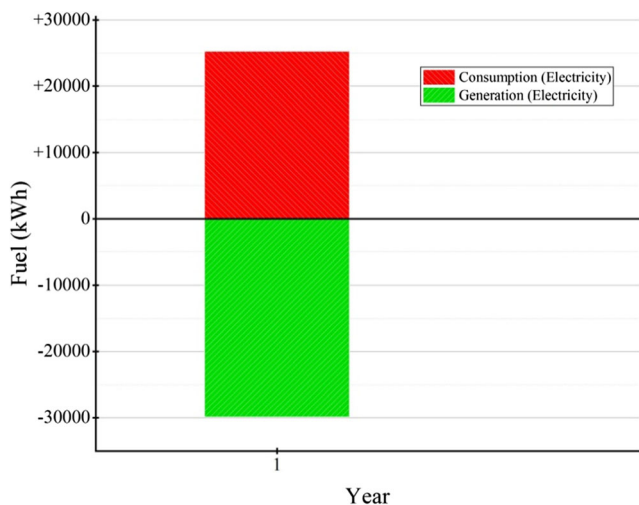


Fig. 7 Overall annual energy consumption and energy generation using renewable energies in the zero-energy building

where T represents the temperature; i and o coefficients show the internal and external surfaces, respectively; t represents the time in one stage; and Z , Y , and Ψ show the internal, cross, and flux coefficients.

The amount of the energy required for consumption of 1 year to cool the interior space of the building in terms of $\text{kWh/m}^2 \cdot \text{year}$ is determined by Eq. 4:

$$CN_{usf} = \frac{1-\eta_c}{A} \times Q_{gn,c} \tag{4}$$

where η_c , A , and $Q_{gn,c}$ represent the loss coefficient in the cooling system, the total net cooled area of the building, and the total flux of the internal and solar heat gain of the building.

As seen in the “building model” section, the cooling temperature should be set on a certain amount for some seasons of

the year to be able to solve this equation. $Q_{gn,c}$ is figured out by Eq. 5:

$$Q_{gn,c} = Q_{opq} + Q_s + Q_i \tag{5}$$

where Q_{opq} is the internal temperature caused by equipment, lights, and building occupants; Q_s represents the solar heat gained from transparent environments (e.g., windows and other transparent surfaces); and Q_i shows the solar heat gained from opaque environments.

Finally, heat loss through exterior walls is figured out by Eq. 6:

$$Q_{loss} = U(T_i - T_{md}) \tag{6}$$

where U , T_i , and T_{md} represent the overall temperature transfer coefficient, the fixed internal temperature, and the mean daily temperature, respectively, with T_{md} being figured by Eq. 7:

$$T_{md} = \frac{T_{rad} + T_{air}}{2} \tag{7}$$

where T_{rad} and T_{air} represent the radiative temperature and air temperature, respectively.

Calculation of the amount of carbon emissions in a building

Total carbon emissions in construction of a building (E_c) is figured out by Eq. 8 (Patil and Kumthekar 2016):

$$E_c = \sum E_{mat} + \sum E_{trans} + \sum E_{site} + \sum E_{waste} \tag{8}$$

where E_{mat} is the carbon emitted from the building materials, E_{trans} resulted from the carbon emitted during transfer, E_{site} is

Table 5 The building blocks and carbon dioxide produced

Materials embodied carbon and inventory	Area (m ²)	Mass (kg)	Embodied carbon (kg.CO ₂)	Equivalent CO ₂ (kg.CO ₂)
Painted oak	4.4	107.5	0.0	0.0
Timber flooring	100.0	1950.0	897.0	916.5
Floor/roof screed	100.0	8400.0	1344.0	1344.0
Plasterboard	100.0	3640.0	1383.2	1456.0
Gypsum plastering	204.0	2651.8	1007.7	1060.7
Urea formaldehyde foam	100.0	132.7	236.2	254.8
MW glass wool (rolls)	100.0	173.4	265.3	291.3
XPS extruded polystyrene - CO ₂ blowing	204.0	567.6	1634.6	5437.5
Concrete block (Medium)	204.0	28,557.8	2284.6	2284.6
Cast concrete	100.0	20,000.0	1600.0	1600.0
Cast concrete (dense)	70.0	14,700.0	1176.0	1176.0
Brickwork outer	204.0	34,677.3	7629.0	7975.8
Asphalt 1	100.0	2100.0	105.0	105.0
Subtotal	–	117,658.0	19,552.7	23,912.3

Table 6 The local shape of building and carbon dioxide produced

Glazing embodied carbon and inventory	Area (m ²)	Embodied carbon (kg.CO ₂)	Equivalent CO ₂ (kg.CO ₂)
Project external glazing	50.6	946.8	946.8
Local shading	–	2531.4	2531.4
Window shading	–	2531.4	2531.4
Subtotal	50.6	6009.7	6009.7

caused by carbon emissions through the site, and E_{waste} is the amount of carbon emitted through waste.

Equation 9 yields the carbon emitted through building materials:

$$E_{mat} = Q_{mat} \times EF_{mat} \tag{9}$$

where Q_{mat} represents the quantity of the materials and products made in the building, and EF_{mat} represents the coefficient of materials and products.

Moreover, the overall annual carbon emissions, E_{o-a} , are caused by the function of the building at the time of operation with electricity consumption:

$$E_{o-a} = E_{ele-a} \tag{10}$$

$$E_{ele-a} = C_{ele-a} \times EF_{grid} \tag{11}$$

where E_{ele-a} shows the carbon emissions due to the annual consumption of electrical energy, C_{ele-a} represents the annual electrical energy consumption, and EF_{grid} shows the carbon emissions coefficient for generation and distribution of electricity.

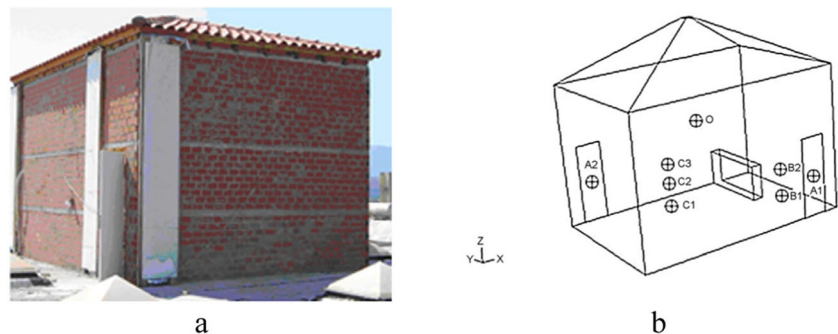
Results

According to Eqs. 1 to 7, Fig. 5 illustrates the results of energy analysis on the administrative building in different months of a year. This figure allows comparing consumed energies, either thermal or electrical. As can be seen, some of the energies (lighting, electrical equipment, etc.) are relatively constant and others are variable according to the utilization of building in seasons. For example, lighting electrical systems (including

computers and other electronic equipment) was constant throughout the year and cooling equipment was variable, which was active only during summer. Figure 6 illustrates the details of the monthly electrical energy consumption for a building which uses both a photovoltaic panel and a wind turbine, including solar lighting, the electrical energy used for lighting, the electrical energy consumed for cooling, and the electrical energy consumed for water heating, excluding the electrical energy used for occupants’ activities and all equipment. As stated earlier, and considering the climate in Zahedan City, most energy consumption is due to the energy used for cooling in hot seasons of the year, in a way that the largest cooling load for this building was in June, amounting 1227 kWh. The annual quantities of electrical energy used for the activities of the occupants of this building and all equipment, excluding lighting, electrical energy used for lighting, electrical energy used for cooling, and the electrical energy used for water heating, were 6457.8 kWh, 9345.8 kWh, 8869.2 kWh, and 586.5 kWh, respectively, while annual electrical energy generation was 27,318.4 kWh. Finally, Fig. 7 compares the load of the annual electrical consumption of the building and the annual electricity generated by renewable energies. In fact, this figure is indicative of the fact that the overall annual energy generation of the building (resulted from the photovoltaic panels mounted on the building roof as well as the wind turbine) was slightly larger than the annual energy consumption of this building. Therefore, regarding energy consumption, this building has become zero-energy.

Table 5 shows the figures for the occupied area, mass, embodied CO₂, and emitted CO₂ for each of the materials used in the modeled building. As it is observed, the overall carbon is 19,552.7 kg and the equivalent CO₂ is 23,912.3 kg.

Fig. 8 Real building for numerical validation: **a** physical model and **b** measured point positions (Stavarakakis et al. 2008)



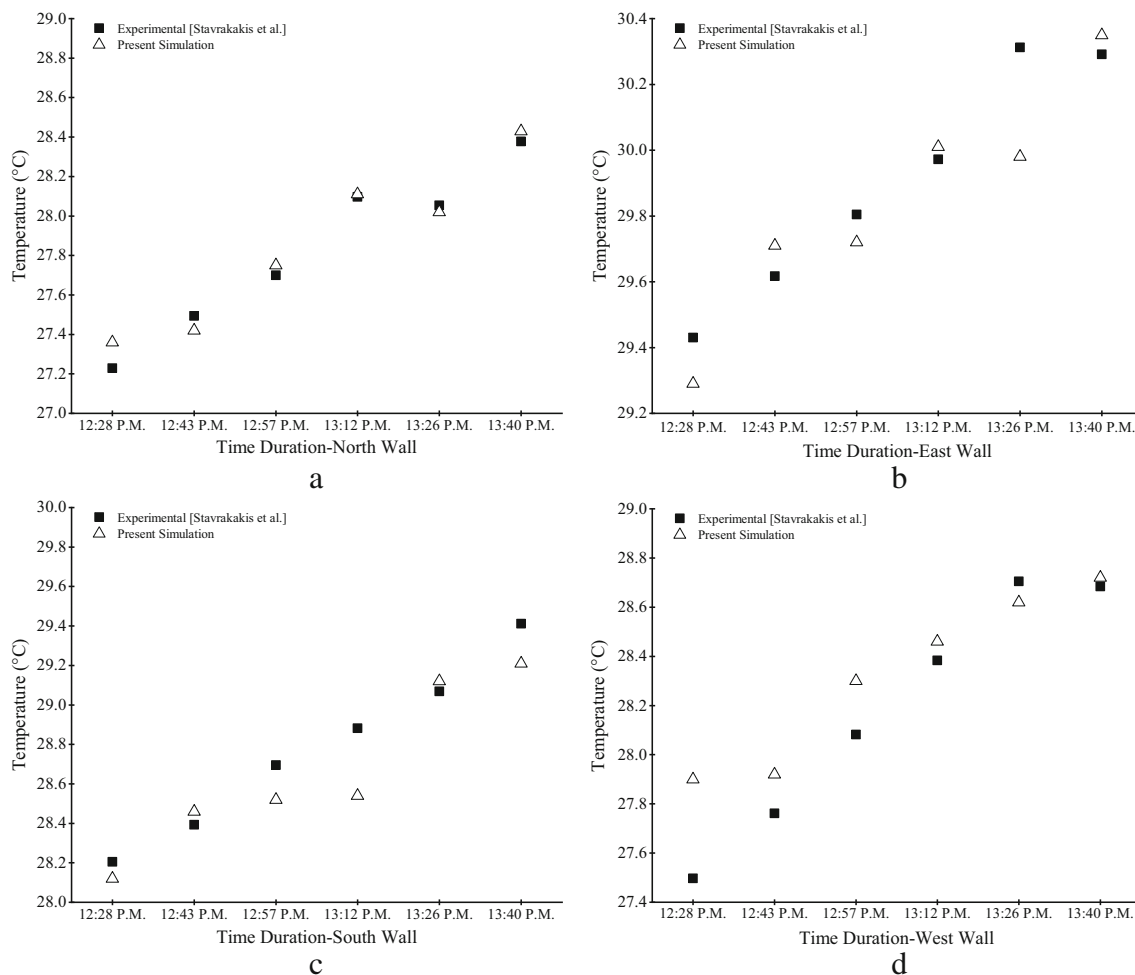


Fig. 9 Comparison between simulation results and experimental data—average surface temperature of the wall in four orientations: **a** north orientation, **b** east orientation, **c** south orientation, and **d** west orientation

The amount of carbon emitted through external glazing, window shading, etc. is also tabulated in Table 6.

Eventually, the embodied CO₂ of 25,582.3 kg and equivalent CO₂ of 29,921.8 kg were yielded for the total building area of 529 m².

Discussion

Reducing energy consumption in buildings is a major global goal as the world moves towards designing sustainable buildings. Building components, especially envelopes, are the first energy consumers, and buildings have a wide range of walls, and window openings on the wall represent the main energy consumption and sustainability factor.

In the present study, in order to ensure the accuracy of the simulation results, some results have been compared and validated with experimental data which were mentioned in the literature review (Stavrakakis et al. 2008). The physical model

of the tested building of dimensions 6 m × 4 m × 5.5 m is seen in Fig. 8. In Fig. 8a, a photograph of the studied building is shown, and in Fig. 8b, a schematic diagram of the measurement points of one-dimensional velocity and temperature has been given. Points B2 and C3 are located inside the building and point A2 is located in the middle of the north door. In Fig. 9(a to d), for four different types of building orientation, the average surface temperature of each wall is obtained, and the results indicate a good agreement between the measured temperatures and the present simulation. Also in Fig. 10, the experimental data for one-dimensional velocity of three points (A2, B2, and C3) is compared with the present study. As can be seen, there is still a good agreement between the present simulation and experimental data.

The current research method to evaluate energy performance in buildings and reduce environmental pollution is the use of architectural solutions for designing openings. The effect of building orientation changes (north, east, south, and west) and window to wall ratio (WWR 20, 30, and 40%) to achieve these goals has been investigated. Changing these

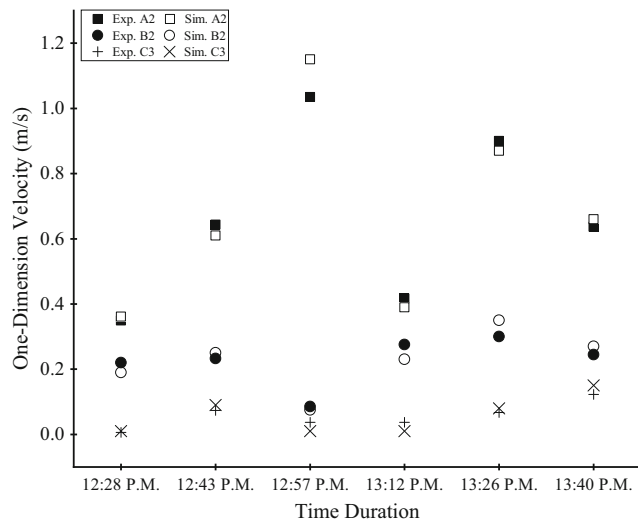


Fig. 10 Comparison between simulation results and experimental data—velocity in three points

parameters in hot and cold seasons of the year creates 96 different scenarios. The effect of changes in these scenarios on operative temperature, discomfort hours of occupants, and emission of carbon dioxide has been studied. Figure 11

illustrates the four main orientations of the building on August 23 at 10 A.M.

Impact on operative temperature

Operative temperatures in winter and summer are good indicators of the energy consumption of air conditioning systems and the index of thermal comfort (Table 7 in the Appendix) for building occupants. In this section, the effect of two parameters (WWR and different building orientations) in August and January on average operative temperature is shown in Figs. 12a and b, respectively. As can be seen in Fig. 12a, unlike the cooler months of the year, in August, there are many fluctuations in the operative temperature diagram of the building in different orientations, so that the lowest operative temperature in WWR 20% is in the west orientation of the building and the highest operative temperature is in WWR 40% for northeast orientation. However, in the southern direction of the building, the operating temperature is still high, and in any case, as the WWR increases in all directions, the operative temperature also increases in the warm seasons, due to the increase in the intensity of solar radiation received through

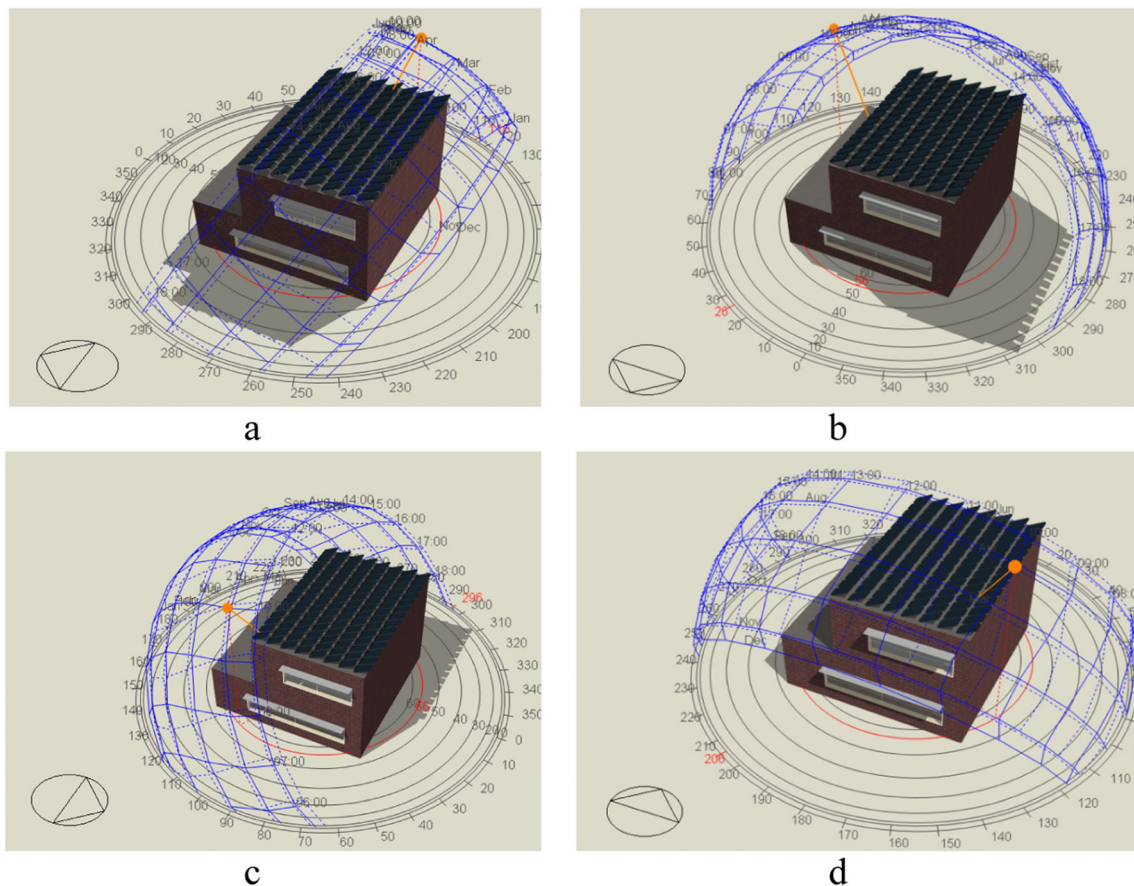
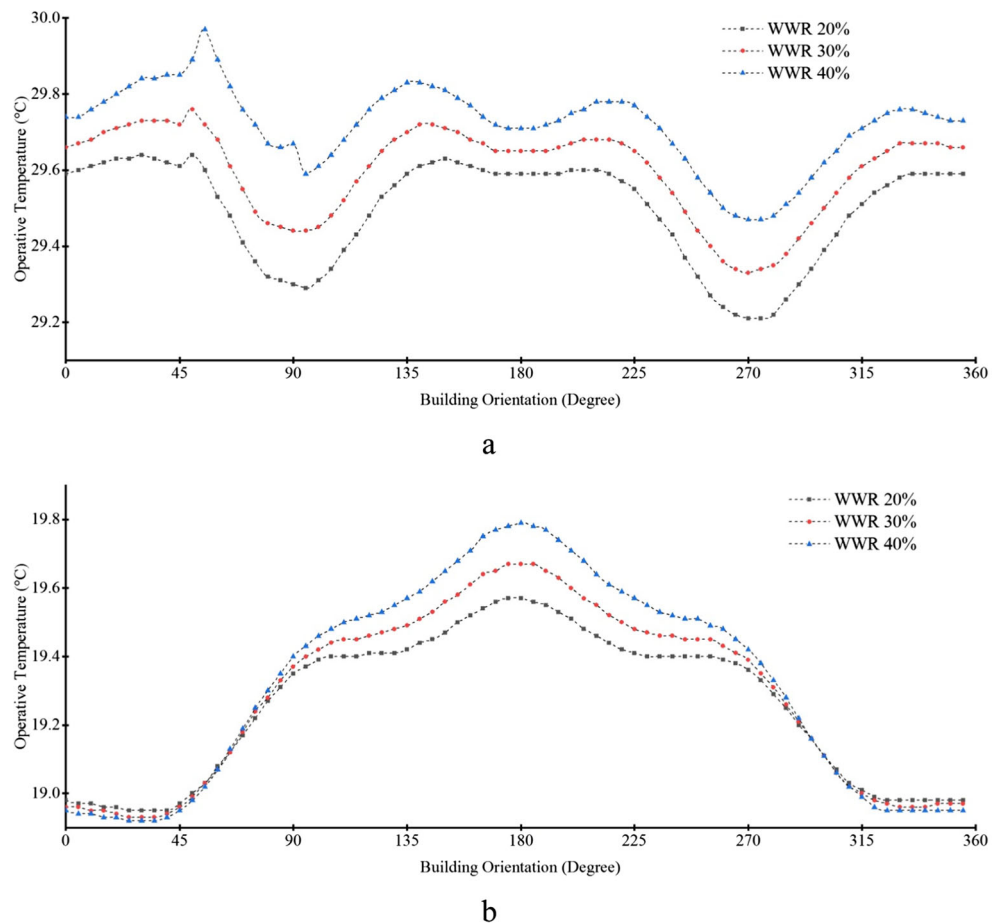


Fig. 11 Different orientations of the modeled building on August 23 at 10 A.M.: **a** north orientation, **b** east orientation, **c** south orientation, and **d** west orientation

Fig. 12 Monthly operative temperature with various WWR and building orientation: **a** August and **b** January



windows. But in January (Fig. 12b), the trend of operative temperature diagram is more regular and it is observed that in the south orientation of the building, with WWR 40%, and the highest operative temperature (19.8 °C) and the lowest operative temperature are related to the north orientation (18.9 °C) with WWR 40% too. These results can be more important in passive buildings that are actually energy efficient.

Impact on discomfort hours

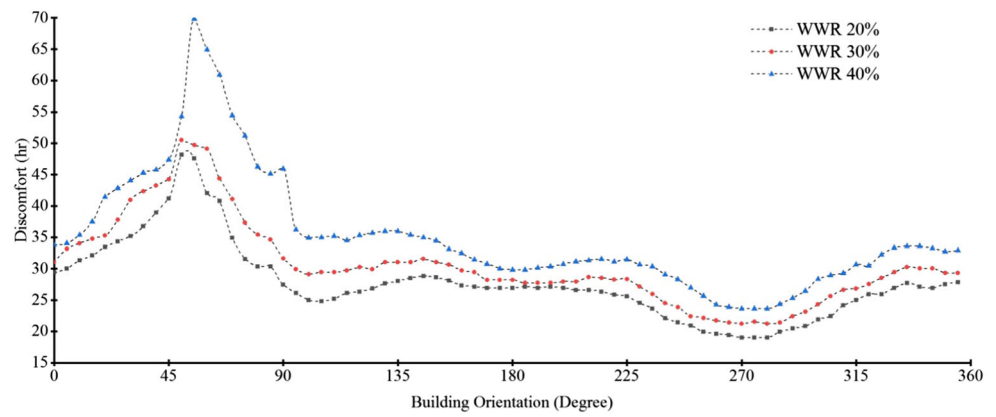
Figure 13(a and b) shows the effect of WWR and building orientation on discomfort hours that the air conditioning system needs to operate in August (summer) and January (winter), respectively. As can be seen in Fig. 13, the discomfort hours in summer are more than those in winter, generally, which is due to the warmer ambient air temperature in hot climates. In summer (Fig. 13a), the maximum discomfort hour for WWR 40% is in the northeast orientation and the maximum comfort hour for WWR 20% is in the west orientation. In winter (Fig. 13b), the south orientation has the minimum discomfort (35 h), because, in this season, the south orientation has the highest amount of

incident solar radiation. For this reason, the northwest orientation has the longest discomfort hours (about 87 h) in winter compared with other orientations. Therefore, in winter, the amount of WWR 40% is better with the south orientation and in summer, WWR 20% is the best with the west orientation. In Fig. 14, it is shown that in the annual analysis, which can be a more important decision in the design and construction of an energy-efficient building, the south orientation is a priority. The building with WWR 40% in south orientation has a total of 160 h of discomfort. In other words, in the annual evaluation of the thermal comfort of the building occupants, the best window to wall ratio is 40% in the south orientation, and the northeast orientation has maximum discomfort hours with WWR 40%. Of course, it should be noted that if the building was designed in the east and northeast orientation, the best amount of WWR is 20%.

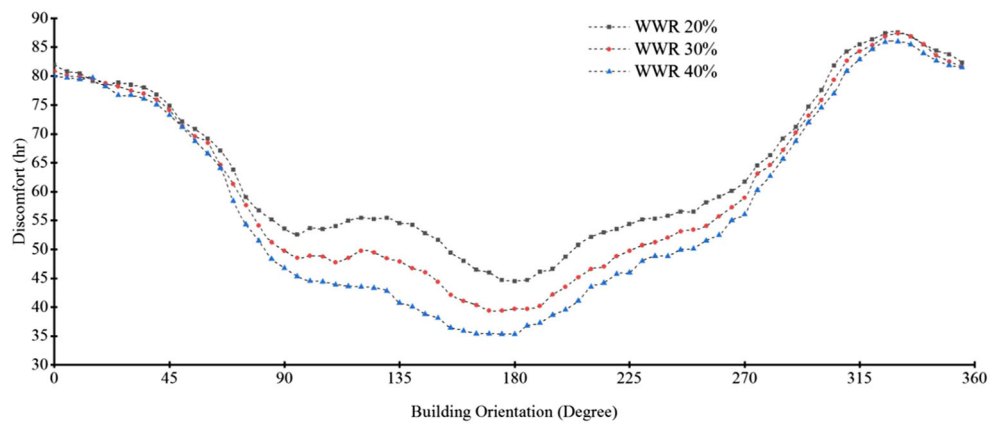
Impact on CO₂ emissions

With passive solar methods, up to 17% reduction in emitted gases that plays an important role in electricity generation is possible (Mahdavi Adeli et al. 2019). In Fig. 15a, in terms of

Fig. 13 Monthly discomfort hours with various WWR and building orientation: **a** August and **b** January



a



b

CO₂ production, in the warm months of the year, the best orientation is in the west with WWR 20%, followed by the east orientation, and the worst orientation is the southeast orientation with CO₂ production of 1347 kg and with WWR 40%. In the

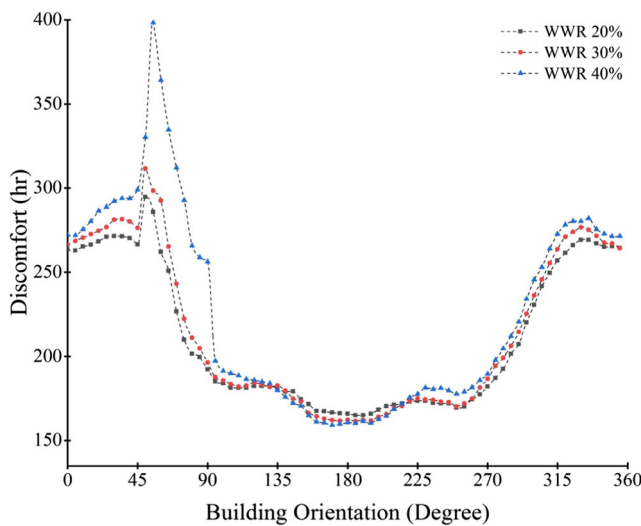


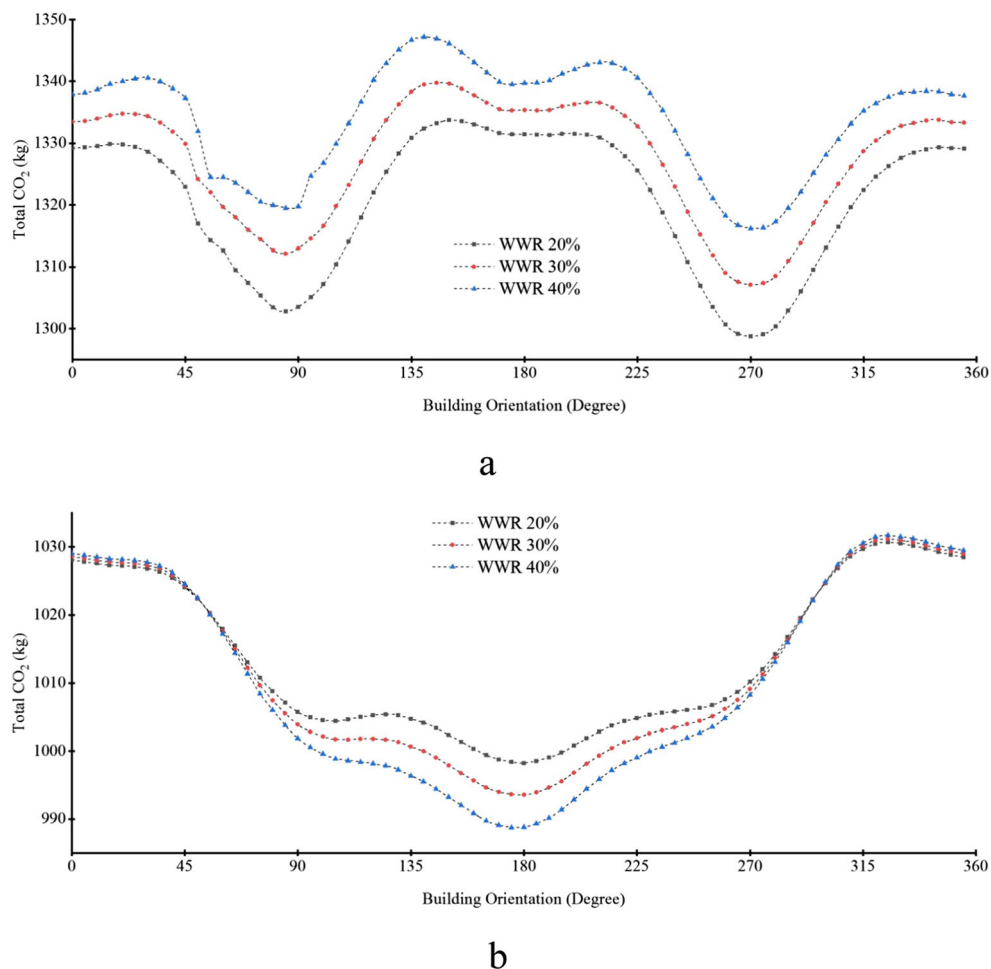
Fig. 14 Annual discomfort hours with various WWR and building orientation

cold months of the year (Fig. 15b), the lowest amount of carbon dioxide production is 988 kg and the southern direction has lower energy consumption due to the use of natural solar energy to heat the building in this direction. It should be noted that the amount of carbon dioxide emitted is related to the energy consumption of the building. As can be seen in Fig. 16, the effect of the window to wall ratio and building orientation is shown in the annual amount of CO₂ emitted. In the annual analysis, the priority is on the east orientation with WWR 20% and then the west orientation with WWR 20%. The worst-case scenario occurs with the production of 12,891 kg of carbon dioxide, a WWR 40%, and a northwest orientation. Although in the cold seasons of the year the WWR 40% produces less carbon dioxide (Fig. 15b), in total, the annual analysis (Fig. 16) shows that WWR 20% compared with WWR 30% and 40% will produce less amount of CO₂.

Conclusion

As about 30–40% of energy demands in most developed countries or developing countries come from the construction sector, thus, buildings are regarded as the main

Fig. 15 Monthly CO₂ emissions with various WWR and building orientation: **a** August and **b** January



key to shifting to sustainability in the energy sector. Considering the high electricity consumption in buildings, these figures often rise to over 40% in the primary energy and in energy related to CO₂ emissions. In

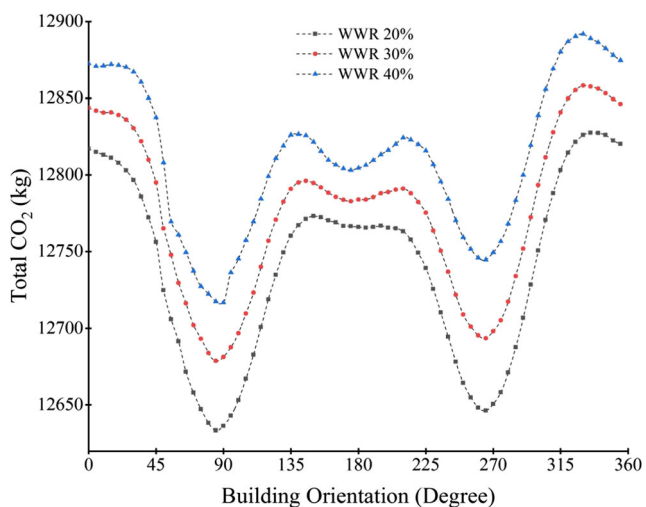


Fig. 16 Annual CO₂ emissions with various WWR and building orientation

summary, energy generation depends on energy generation sources and the essential extraction methods for the exploitation of energy sources. Energy generation is directly dependent on human needs, and energy consumption can be related to the economic growth of a society and the society itself. Nowadays, energy demand is larger than ever. Unfortunately, more than 84% of our energy at present is generated from fossil resources which are finite and non-renewable. Therefore, the need for the development of energy generation sources, technologies, and new techniques becomes more vital day by day. Conservation of energy is the main concern in the efforts for energy sustainability. Thus, the exploitation of fossil fuels can be reduced by choosing the optimum building form.

The presence of windows in the façade of the buildings is essential for ventilation and lighting. While increasing the size of a window can lead to increased ventilation and lighting, it can also increase the heat received by the incoming solar energy and increasing heat absorption or loss, because the thermal resistance of window glass is lower than the walls of a building and it creates a thermal bridge.

In this study, the parametric analysis showed northeast orientation of 80° and window to wall ratio of 40% were the best building orientations in the reduction of CO₂ production approach, but in the same orientation of the building and in terms of thermal comfort, the building occupants had more than 400 h of discomfort experience, which is significant. The annual analysis shows that carbon dioxide

production in the south orientation is almost constant (120 to 220°) and the rotation of the building at these degrees will have almost no effect on changing the annual CO₂ production of the building. The results also demonstrate that the minimum annual production of carbon dioxide is about 12,633 kg, which can be reduced by about 258 kg, which is a significant amount.

Appendix. Environmental and thermal comfort data for different seasons

Table 7 Site data and comfort for different months of the year

Data	Months											
	Jan	Feb	Mar	Apr	May	Jun	Jul	Aug	Sep	Oct	Nov	Dec
Air temperature	23.7	24.2	25.7	26.9	29.1	30.7	31.4	31.8	30.4	27.8	25.5	23.7
Radiant temperature	24.9	25.6	27.3	29.1	31.4	32.8	33.6	33.7	32.5	29.8	27.1	24.8
Operative temperature	24.3	24.6	26.5	28.0	30.2	31.7	32.5	32.8	31.5	28.8	26.3	24.3
Outside dry-bulb temp. (°C)	17.9	19.1	23.2	26.6	30.6	33.0	34.2	33.3	32.0	28.8	23.4	18.5
Outside dew-point temp. (°C)	9.4	12.0	15.5	18.2	22.3	24.2	26.7	27.2	24.6	20.8	13.5	11.8
Wind speed (m/s)	2.2	2.3	3.2	2.4	3.3	2.9	3.7	4.1	3.2	1.6	2.1	2.8
Wind direction (°)	107.3	131.2	128.5	108.0	126.8	131.2	130.3	135.3	143.5	68.4	123.6	144.7
Solar altitude (°)	-13.0	-8.3	-1.3	6.2	11.8	14.3	13.2	8.8	2.0	-5.5	-11.5	-14.2
Solar azimuth (°)	189.8	190.2	191.8	193.9	194.9	194.2	193.0	193.2	194.7	195.8	194.5	191.1
Atmospheric pressure (kPa)	101.5	101.4	101.3	101.0	100.5	99.8	99.5	99.6	99.9	100.2	100.8	101.1
Direct normal solar (kWh)	108.5	104.8	135.9	114.9	119.3	163.6	123.2	139.9	117.3	106.8	95.2	95.0
Diffuse horizontal solar (kWh)	103.1	131.3	121.8	183.7	196.7	156.6	158.1	147.5	156.3	139.0	111.8	98.0

References

- Alwetaishi M, Taki A (2019) Investigation into energy performance of a school building in a hot climate: optimum of window-to-wall ratio. *Indoor Built Environ* 0(0):1–16. <https://doi.org/10.1177/1420326X19842313>
- Azari R et al. (2016) ‘Multi-objective optimization of building envelope design for life cycle environmental performance’, *Energ Buildings*. Elsevier B.V. doi: <https://doi.org/10.1016/j.enbuild.2016.05.054>
- Beyhan B, Cellat K, Konuklu Y, Gungor C, Karahan O, Dunder C, Paksoy H (2017) Robust microencapsulated phase change materials in concrete mixes for sustainable buildings. *Int J Energy Res* 41(January 2017):113–126. <https://doi.org/10.1002/er.3603>
- Cellat K, Beyhan B, Güngör C, Konuklu Y, Karahan O, Dunder C, Paksoy H (2015) Thermal enhancement of concrete by adding bio-based fatty acids as phase change materials. *Energ Buildings*. Elsevier 106:156–163. <https://doi.org/10.1016/J.ENBUILD.2015.05.035>
- Cellat K, Beyhan B, Konuklu Y, Dunder C, Karahan O, Güngör C, Paksoy H (2019) 2 years of monitoring results from passive solar energy storage in test cabins with phase change materials. *Sol Energy Pergamon* 200:29–36. <https://doi.org/10.1016/J.SOLENER.2019.01.045>
- Charles A, Meref W, Ouellet-plamondon CM (2018) Case study of the upgrade of an existing office building for low energy consumption and low carbon emissions. *Energ Buildings*. Elsevier B.V. <https://doi.org/10.1016/j.enbuild.2018.10.008>
- EnergyPlus (2016) ‘The board of US Department of Energy (DOE). October 1, (2013).’, *EnergyPlus Engineering Reference*
- Feng G et al (2017) ScienceDirect ScienceDirect study on the influence of window-wall ratio on the energy consumption of nearly zero energy buildings. *Proc Eng*. Elsevier B.V. 205:730–737. <https://doi.org/10.1016/j.proeng.2017.10.003>
- Harmati N, Magyar Z (2015) Influence of WWR, WG and glazing properties on the annual heating and cooling energy demand in buildings. *Energy Procedia*. Elsevier B.V. 78:2458–2463. <https://doi.org/10.1016/j.egypro.2015.11.229>
- Kwon HJ, Yeon SH, Lee KH, Lee KH (2018) Evaluation of building energy saving through the development of venetian blinds optimal control algorithm according to the orientation and window-to-wall ratio. *Int J Thermophys Springer US*. <https://doi.org/10.1007/s10765-017-2350-3>
- Lobaccaro G et al. (2018) ‘PT’, *Energ Buildings*. Elsevier B.V. doi: <https://doi.org/10.1016/j.enbuild.2018.02.025>
- Mahdavi Adeli M et al (2011) Experimental exergetic performance evaluation of a photovoltaic thermal (PV/T) air collector and comparison with numerical simulation. *Proc Inst Mech Eng E J Process Mech Eng* 225(3):161–172. <https://doi.org/10.1177/09544089JPM371>
- Mahdavi Adeli M et al (2012) Experimental performance evaluation of a photovoltaic thermal (PV/T) air collector and its optimization. *Stroj Vestn-J Mech E* 58(5):309–318. <https://doi.org/10.5545/sv-jme.2010.007>
- Mahdavi Adeli M, Farahat S, Sarhaddi F (2017) Analysis and optimization using renewable energies to get net-zero energy building for warm climate. *J Comput Appl Mech* 48(2):331–344. <https://doi.org/10.22059/jcamech.2017.240840.182>
- Mahdavi Adeli M, Farahat S, Sarhaddi F (2019) Increasing thermal comfort of a net-zero energy building inhabitant by optimization of energy consumption. *Int J Environ Sci Technol*. Springer Berlin Heidelberg 17(5):2819–2834. <https://doi.org/10.1007/s13762-019-02603-0>
- Mahdavi Adeli M, Farahat S, Sarhaddi F (2020) Optimization of energy consumption in net-zero energy buildings with increasing thermal comfort of occupants. *Int J Photoenergy*, 2020. <https://doi.org/10.1155/2020/9682428>
- Moschetti R, Brattebø H, Sparrevik M (2019) Exploring the pathway from zero-energy to zero-emission building solutions: a case study of a Norwegian office building. *Energ Buildings*. Elsevier B.V. <https://doi.org/10.1016/j.enbuild.2019.01.047>
- Namjoo A, Sarhaddi F, Sobhnamayan F, Alavi MA, Mahdavi Adeli M, Farahat S (2011) Exergy performance analysis of solar photovoltaic thermal (PV/T) air collectors in terms of exergy losses. *J Energy Inst* 84(3):132–145. <https://doi.org/10.1179/174396711X12992532689177>
- Pathirana S, Rodrigo A, Halwatura R (2019) Effect of building shape, orientation, window to wall ratios and zones on energy efficiency and thermal comfort of naturally ventilated houses in tropical climate. *Int J Energy Environ Eng*. Springer Berlin Heidelberg, (0123456789). <https://doi.org/10.1007/s40095-018-0295-3>
- Patil NM, Kumthekar MB (2016) ‘Low carbon building’, *Int Res J Eng Technol*, 3(12)
- Petrichenko K, Ürge-vorsatz D, Cabeza LF (2019) Energy & buildings modeling global and regional potentials for building-integrated solar energy generation. Elsevier B.V., 198, pp. 329–339. doi: <https://doi.org/10.1016/j.enbuild.2019.06.024>
- Sarhaddi F, Farahat S, Ajam H, Behzadmehr A, Mahdavi Adeli M (2010) An improved thermal and electrical model for a solar photovoltaic thermal (PV/T) air collector. *Appl Energy*. Elsevier 87(7):2328–2339. <https://doi.org/10.1016/J.APENERGY.2010.01.001>
- Stavarakakis GM, Koukou MK, Vrachopoulos MG, Markatos NC (2008) Natural cross-ventilation in buildings: building-scale experiments, numerical simulation and thermal comfort evaluation. *Energ Buildings* 40(9):1666–1681. <https://doi.org/10.1016/j.enbuild.2008.02.022>
- Su X, Zhang X (2010) Environmental performance optimization of window – wall ratio for different window type in hot summer and cold winter zone in China based on life cycle assessment. *Energ Buildings* 42:198–202. <https://doi.org/10.1016/j.enbuild.2009.08.015>
- Syngros G, Balaras CA, Koubogiannis DG (2017) Embodied CO₂ emissions in building construction materials of Hellenic dwellings. *Procedia Environ Sci*. The author(s) 38:500–508. <https://doi.org/10.1016/j.proenv.2017.03.113>
- Valizadeh M, Sarhaddi F, Mahdavi Adeli M (2019) Exergy performance assessment of a linear parabolic trough photovoltaic thermal collector. *Renew Energy*. Pergamon 138:1028–1041. <https://doi.org/10.1016/J.RENENE.2019.02.039>
- Yazdanpanahi J, Sarhaddi F, Mahdavi Adeli M (2015) Experimental investigation of exergy efficiency of a solar photovoltaic thermal (PVT) water collector based on exergy losses. *Sol Energy*. Pergamon 118:197–208. <https://doi.org/10.1016/J.SOLENER.2015.04.038>
- Zomorodian ZS, Tahsildoost M (2018) Energy and carbon analysis of double skin façades in the hot and dry climate. *J Clean Prod*. Elsevier Ltd 197:85–96. <https://doi.org/10.1016/j.jclepro.2018.06.178>

Publisher’s note Springer Nature remains neutral with regard to jurisdictional claims in published maps and institutional affiliations.